Materials Transactions, Vol. 49, No. 6 (2008) pp. 1446 to 1450

Annealing of Amorphous Sm_5Fe_{17} Melt-Spun Ribbon

Tetsuji Saito

Department of Mechanical Science and Engineering, Chiba Institute of Technology, Narashino 275-0016, Japan

An amorphous Sm_5Fe_{17} melt-spun ribbon was annealed under various conditions to obtain the metastable Sm_5Fe_{17} phase. The Sm_5Fe_{17} phase could be obtained by annealing at temperatures between 873 K and 973 K for 0.1–1 h. However, the annealed specimens contained other phases such as the $SmFe_2$ and $SmFe_3$ phases depending on the annealing conditions. It was found that the specimen annealed at 873 K for 1 h consisted mostly of the Sm_5Fe_{17} phase. The Sm_5Fe_{17} phase could also be obtained by annealing the amorphous Sm_5Fe_{17} melt-spun ribbon at 1073 K for 0.1 h or 0.3 h, but annealing at that temperature for 1 h resulted in decomposition of the metastable Sm_5Fe_{17} phase and formed the equilibrium Sm_2Fe_{17} and $SmFe_3$ phases. [doi:10.2320/matertrans.MBW200781]

(Received October 16, 2007; Accepted March 4, 2008; Published May 25, 2008)

Keywords: *samarium-iron alloys, melt-spinning, amorphous alloys, magnetic properties*

1. Introduction

With the advent of high-energy-product Nd-Fe-B permanent magnets, research and development of new permanent magnet materials has mainly been concentrated on rare-earth-containing alloys.[1,2] As a consequence of intensive research on such alloys, it has been found that the Nd_5Fe_{17} phase is the stable intermetallic compound in the binary Nd-Fe system.[3–5] Although the Nd_5Fe_{17} phase has a high saturation magnetization of 1.61 T at 4 K and a Curie temperature above 500 K, it does not possess c-axis anisotropy, which is essential for permanent magnet materials.[6] Since Sm has a Stevens factor αj with a different sign from that of Nd, the Sm_5Fe_{17} phase is expected to show c-axis anisotropy. The formation of the Sm_5Fe_{17} phase has been reported in sputtered films, which exhibited a large coercivity of 1.12 MAm^{-1}.[7,8] It is found, however, that the Sm_5Fe_{17} phase can be produced by annealing an amorphous Sm-Fe melt-spun ribbon.[9] At that time, the Sm_5Fe_{17} phase was believed to be the stable phase as was the case for the Nd_5Fe_{17} phase. Recent studies have revealed that the Sm_5Fe_{17} phase is the metastable phase and can only be obtained by an annealing amorphous Sm-Fe melt-spun ribbon.[10] The magnetic studies indicate that Sm-Fe melt-spun ribbons with the Sm_5Fe_{17} phase exhibit high coercivity exceeding 2.8 MAm^{-1}.[11]

For the formation of permanent magnets from the amorphous phase controlled crystallization of the amorphous melt-spun material is a prerequisite for the attainment of sufficiently large coercivity. There have been many studies on the annealing conditions of the rapidly solidified Nd-Fe-B alloys.[12,13] Unlike in the case of Nd-Fe-B magnets, the hard magnetic Sm_5Fe_{17} phase is a metastable phase. Such a metastable phase can be obtained only when the kinetically preferred course differs from the course most favored thermodynamically.[14,15] It is therefore significant to investigate the crystallization behavior of the amorphous material when endeavoring to obtain the metastable phase. The focus of this study was the crystallization behavior of an amorphous Sm-Fe melt-spun ribbon having the composition of Sm_5Fe_{17}. The thermal stability and crystallization phases of the amorphous and annealed Sm-Fe melt-spun ribbon were intensively examined by thermomagnetic measurements.

2. Experimental

Sm-Fe alloy ingots were prepared by induction melting of Sm (99.9 mass%) and iron (99.9 mass%) under an argon atmosphere. An alloy ingot of 20 g was induction melted under an argon atmosphere in a quartz crucible having an orifice 0.6 mm in diameter at the bottom. The molten metal was ejected through the orifice with argon onto a chromium-plated copper wheel rotating at a surface velocity of 50 ms^{-1}. The melt-spun ribbon wrapped with tantalum foil was annealed under an argon atmosphere for 0.1–1 h at temperatures between 773 K and 1073 K. The composition of the melt-spun ribbon was examined by chemical analysis using inductively coupled plasma (ICP). The phases of the specimens were examined by X-ray diffraction (XRD) using Cu Kα radiation. The temperature dependence of the magnetization was examined in a helium atmosphere at an applied field of 40 kAm^{-1} by a vibrating sample magnetometer (VSM). Thermomagnetic analysis (TMA) of the specimens was also carried out in an argon atmosphere at an applied field of 8 kAm^{-1} by a thermomagnetic balance.

3. Results and Discussion

Figure 1 shows the XRD pattern of the melt-spun ribbon. The composition of the melt-spun ribbon was identified to be Fe-22.6 at%Sm by chemical analysis. The Sm content of the melt-spun ribbon is comparable to the stoichiometric content (22.7 at%Sm). According to the phase diagram, a Sm_5Fe_{17} alloy at equilibrium locates in the region of two phases: Sm_2Fe_{17} and $SmFe_3$.[16] However, the XRD pattern of the melt-spun ribbon shows no evidence of these peaks, but instead exhibits a broad maximum at around 40 degrees. Only a broad halo peak is found, suggesting that the high solidification rate of melt-spinning results in the formation of the amorphous phase.

It is known that the crystallization behavior of materials from the amorphous state is deeply dependant on the

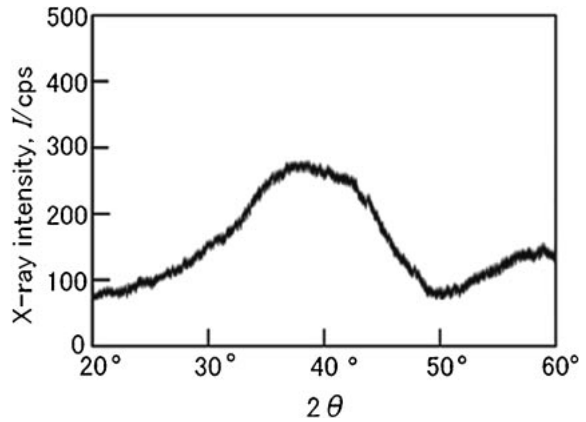

Fig. 1 XRD pattern of the Sm_5Fe_{17} melt-spun ribbon.

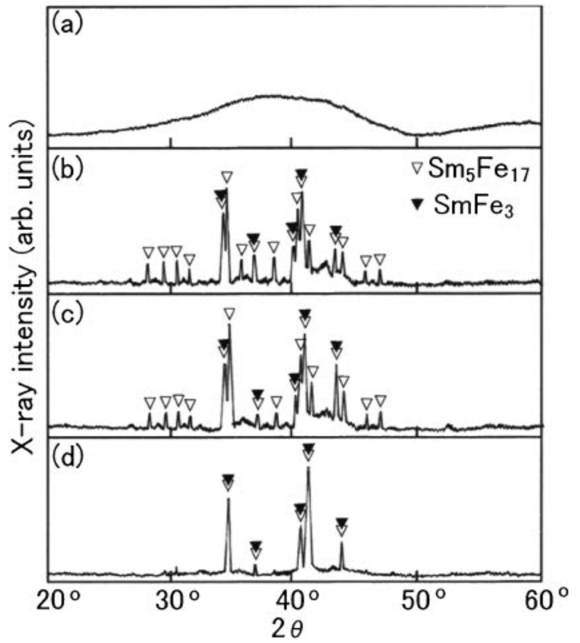

Fig. 2 XRD patterns of the amorphous Sm_5Fe_{17} melt-spun ribbon annealed for 1 h at (a) 773 K, (b) 873 K, (c) 973 K, and (d) 1073 K.

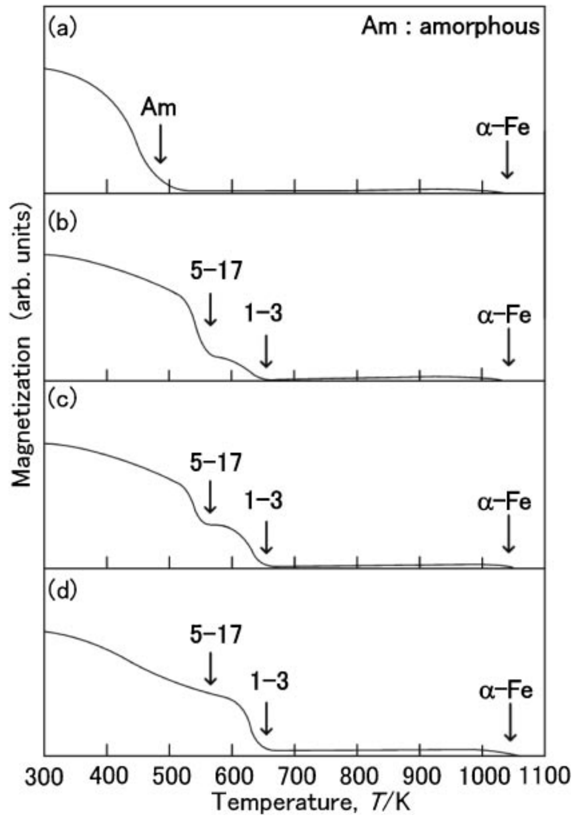

Fig. 3 Temperature dependence of the magnetization of the Sm_5Fe_{17} melt-spun ribbon annealed for 1 h at (a) 773 K, (b) 873 K, (c) 973 K, and (d) 1073 K.

annealing time and temperature. Thus, the amorphous Sm_5Fe_{17} melt-spun ribbon specimens were annealed at temperatures between 773 K and 1073 K for 0.1–1 h. Heat treatment of the ribbons by annealing resulted in changes in the structures and magnetic properties. Figure 2 shows the XRD patterns of the melt-spun ribbon annealed for 1 h at temperatures between 773 K and 1073 K. No clear diffraction peaks are observed in the XRD pattern of the specimen annealed at 773 K. Only a broad halo peak is found, suggesting that the specimen annealed at 773 K is amorphous. The diffraction peaks of the specimen annealed at 873 K match those of the Sm_5Fe_{17} phase, suggesting that this specimen consists of the Sm_5Fe_{17} phase. The presence of the $SmFe_3$ phase has been reported in Sm-Fe system alloys.[16] Since the diffraction peaks of the Sm_5Fe_{17} phase overlap those of the $SmFe_3$ phase, it is difficult to eliminate the possibility that the $SmFe_3$ phase exists in the annealed specimen. Virtually the same XRD pattern was obtained from the specimen annealed at 973 K. On the other hand, the diffraction peaks of the specimen annealed at 1073 K are quite different from those of the specimen annealed at 973 K. No clear diffraction peaks of the Sm_5Fe_{17} phase are observed in the XRD pattern, whereas all of the observed peaks of the Sm_5Fe_{17} phase overlap those of the $SmFe_3$ phase. It is not clear whether the specimen annealed at 1073 K consists of the Sm_5Fe_{17} phase from the XRD studies.

In order to clarify the existence of the $SmFe_3$ phase, the thermomagnetic curves of the melt-spun ribbon and the specimens annealed for 1 h at temperatures between 773 K and 1073 K were examined. Figure 3 shows the temperature dependence of the magnetization of the annealed melt-spun ribbon. The curve of the specimen annealed at 773 K shows a large magnetic transition at around 500 K. According to the results of the XRD studies, the specimen annealed at 773 K consisted of the amorphous phase. No crystalline phases were detected in the XRD studies. Thus, the magnetic transition at around 500 K corresponds to the Curie temperature of the amorphous Sm-Fe alloy with a composition of Sm_5Fe_{17}. The small increase in magnetization at temperatures exceeding 700 K is due to the crystallization of the α-Fe phase from the amorphous melt-spun ribbon. The thermomagnetic curve of the specimen annealed at 873 K exhibits two magnetic transitions at around 550 K and 650 K. The magnetic transitions at around 550 K and 650 K correspond to the Curie temperature of the Sm_5Fe_{17} and $SmFe_3$ phases, respectively. Virtually the same thermomagnetic curve was obtained from the specimen annealed at 973 K. This confirms the results of the XRD studies. A trace of the magnetic

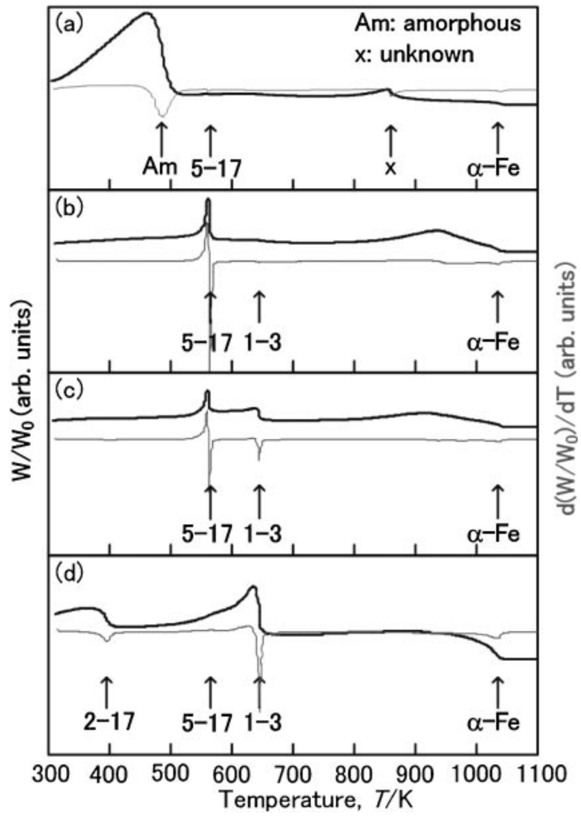

Fig. 4 TMA curves of the amorphous Sm_5Fe_{17} melt-spun ribbon annealed for 1 h at (a) 773 K, (b) 873 K, (c) 973 K, and (d) 1073 K. W/W_o denotes the ratio of the actual weight (W) and original weight (W_o) of the specimen, and $d(W/W_o)/dT$ denotes the divergence of the weight ratio.

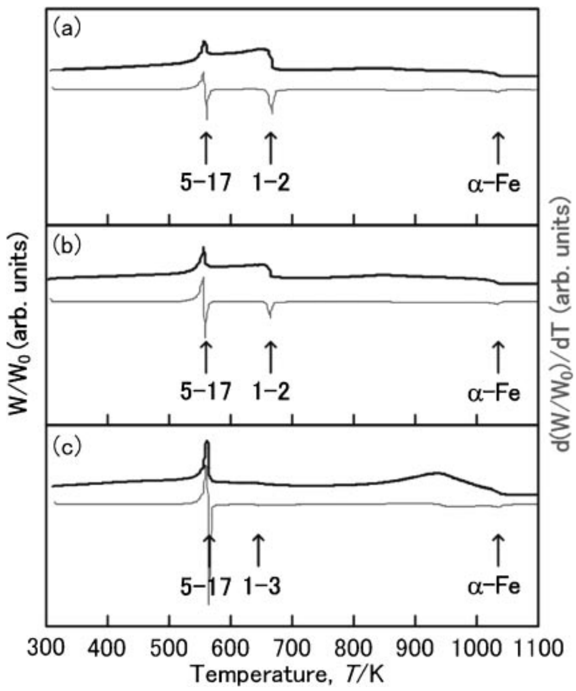

Fig. 5 TMA curves of the amorphous Sm_5Fe_{17} melt-spun ribbon annealed at 873 K for (a) 0.1 h, (b) 0.3 h, and (c) 1 h. W/W_o denotes the ratio of the actual weight (W) and original weight (W_o) of the specimen, and $d(W/W_o)/dT$ denotes the divergence of the weight ratio.

transition at around 550 K is still noticed in the thermomagnetic curve of the specimen annealed at 1073 K, although the magnetic transition is not so clear. A clear magnetic transition at around 650 K is also still seen in the thermomagnetic curve of the specimen annealed at 1073 K, suggesting that this specimen is mostly composed of the $SmFe_3$ phase. It is known that the Sm_5Fe_{17} phase is a metastable phase and that annealing at high temperatures will lead to the formation of the stable phase in this composition of alloys. It was found that the annealing temperature of 1073 K is too high to obtain the metastable Sm_5Fe_{17} phase.

Figure 4 shows the TMA curves of the melt-spun ribbon annealed for 1 h at temperatures between 773 K and 1073 K. The weight change of the specimens is shown as W/W_o, where W is the actual weight of a specimen and W_o is its original weight of the specimen. The divergence of W/W_o is also plotted. The TMA curve of the specimen annealed at 773 K shows the Curie temperature of the amorphous phase, as was the case for the thermomagnetic curve, but at the same time the TMA curve also reveals the existence of a small amount of the Sm_5Fe_{17} phase and an unknown phase in this specimen. On the other hand, although no difference was detected between the specimens annealed at 873 K and 973 K in the XRD and thermomagnetic curves, the TMA curves show that the specimen annealed at 873 K contains less of the $SmFe_3$ phase than the specimen annealed at 973 K. In addition, the TMA curve reveals that the specimen annealed at 1073 K contains some Sm_2Fe_{17} phase together with the $SmFe_3$ and Sm_5Fe_{17} phases. It was found that changes in the magnetic phase can be more effectively determined by TMA using a thermomagnetic balance than by the temperature dependence of the magnetization measured using a VSM. Further studies were therefore carried out by TMA.

One of the parameters that affects the crystallization behavior of amorphous materials is the annealing time. Thus, the phases in the melt-spun ribbon annealed at 873 K for 0.1–1 h were examined by TMA. The results are shown in Fig. 5. No trace of the magnetic transition of the amorphous phase is found in the TMA curve for the specimen annealed at 873 K for 0.1 h. The TMA curve of this specimen shows magnetic transitions of the Sm_5Fe_{17} and $SmFe_2$ phases. The observed magnetic transition of the α-Fe phase is due to crystallization from the amorphous melt-spun ribbon during the TMA analysis. Therefore, the existence of the magnetic transition of the α-Fe phase detected by TMA should not be considered to be a sign of formation of the crystalline α-Fe phase in the melt-spun ribbon, and doesn't warrant further discussion. The above result suggests that the crystallization phases obtained from the amorphous melt-spun ribbon are the $SmFe_2$ and Sm_5Fe_{17} phases. It is known that both the metastable phase and the equilibrium phase can form thermodynamically by annealing of the amorphous material. The $SmFe_2$ phase is found in the TMA curve, suggesting that the formation of the $SmFe_2$ phase is kinetically favored compared to that of the $SmFe_3$ phase in this composition when amorphous melt-spun ribbon is annealed at 873 K for 0.1 h. The amorphous phase was enriched in iron during the crystallization of the $SmFe_2$ phase. The TMA curve of the specimen annealed for 0.3 h shows a smaller magnetic transition of the $SmFe_2$ phase than that of the specimen

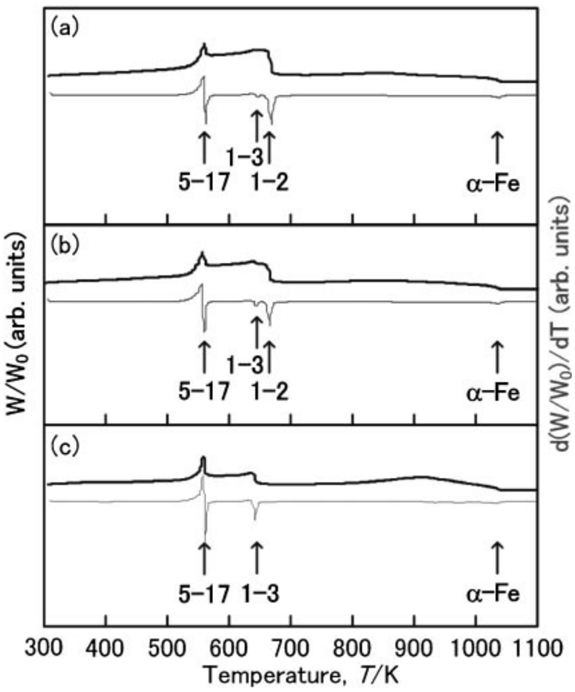

Fig. 6 TMA curves of the amorphous Sm_5Fe_{17} melt-spun ribbon annealed at 973 K for (a) 0.1 h, (b) 0.3 h, and (c) 1 h. W/W_o denotes the ratio of the actual weight (W) and original weight (W_o) of the specimen, and $d(W/W_o)/dT$ denotes the divergence of the weight ratio.

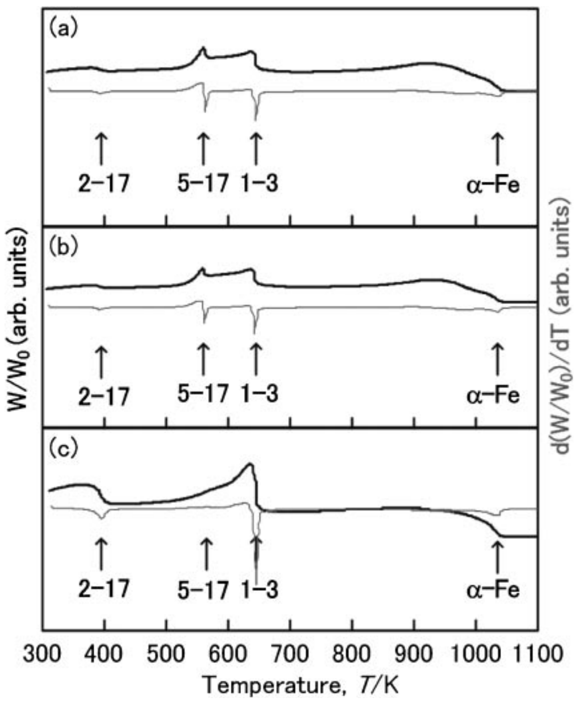

Fig. 7 TMA curves of the amorphous Sm_5Fe_{17} melt-spun ribbon annealed at 1073 K for (a) 0.1 h, (b) 0.3 h, and (c) 1 h. W/W_o denotes the ratio of the actual weight (W) and original weight (W_o) of the specimen, and $d(W/W_o)/dT$ denotes the divergence of the weight ratio.

annealed for 0.1 h. No off-stoichiometric $SmFe_2$ phase is found in the specimen annealed at 873 K for 1 h. A small amount of the equilibrium $SmFe_3$ phase is also formed during the longer annealing.

Figure 6 shows the TMA curves of the amorphous melt-spun ribbon annealed at 973 K for 0.1–1 h. The TMA curve of the specimen annealed at 973 K for 0.1 h shows magnetic transitions of the Sm_5Fe_{17} and $SmFe_2$ phases, similarly to the specimen annealed at 873 K for 0.1 h. However, the TMA curve of the specimen annealed at 973 K for 0.1 h also shows a small magnetic transition of the $SmFe_3$ phase. This indicates that the crystallization phases obtained from the amorphous melt-spun ribbon by annealing at 973 K for 0.1 h are the $SmFe_2$, $SmFe_3$, and Sm_5Fe_{17} phases. The magnetic transition of the $SmFe_2$ phase becomes smaller and disappears as the annealing time increases, while the magnetic transition of the $SmFe_3$ phase becomes progressively larger as the annealing time increases. The fact that no magnetic transition of the $SmFe_2$ phase is seen in the TMA curve of the specimen annealed at 973 K for 1 h confirms that the $SmFe_2$ phase is a non-equilibrium phase.

Figure 7 shows the TMA curves of the amorphous melt-spun ribbon annealed at 1073 K for 0.1–1 h. The specimens annealed at 1073 K for 0.1 h or 0.3 h consist of the Sm_5Fe_{17} and $SmFe_3$ phases, similarly to the specimen annealed at 973 K for 1 h. The difference is that a small magnetic transition of the Sm_2Fe_{17} phase is noted in the specimens annealed for 0.1 h or 0.3 h. A high annealing temperature of 1073 K promotes the formation of the equilibrium Sm_2Fe_{17} and $SmFe_3$ phases. The specimen annealed at 1073 K for 1 h consists mostly of the equilibrium Sm_2Fe_{17} and $SmFe_3$ phases. This indicates that the longer annealing results in the formation of the equilibrium Sm_2Fe_{17} and $SmFe_3$ phases at the expense of the metastable Sm_5Fe_{17} phase.

Table 1 The phases found in annealed Sm_5Fe_{17} melt-spun ribbons determined by TMA.

Annealing condition	Annealed for 0.1 h	Annealed for 0.3 h	Annealed for 1 h
Annealed at 773 K	Amorphous	Amorphous	Amorphous (Sm_5Fe_{17})
Annealed at 873 K	Sm_5Fe_{17} + $SmFe_2$	Sm_5Fe_{17} + $SmFe_2$	Sm_5Fe_{17} ($SmFe_3$)
Annealed at 973 K	Sm_5Fe_{17} + $SmFe_2$ ($SmFe_3$)	Sm_5Fe_{17} + $SmFe_2$ ($SmFe_3$)	Sm_5Fe_{17} + $SmFe_3$
Annealed at 1073 K	Sm_5Fe_{17} + $SmFe_3$ (Sm_2Fe_{17})	Sm_5Fe_{17} + $SmFe_3$ (Sm_2Fe_{17})	Sm_2Fe_{17} + $SmFe_3$ (Sm_5Fe_{17})

Table 1 summarizes the results of the TMA studies. Annealing at 773 K for 0.1–1 h was found to be too low a temperature to obtain the Sm_5Fe_{17} phase. The specimens annealed at 873 K consisted of the Sm_5Fe_{17} phase together with the $SmFe_2$ phase when annealed for 0.1 h or 0.3 h, but consisted mostly of the Sm_5Fe_{17} phase when annealed for 1 h. The specimens annealed at 973 K consisted of the Sm_5Fe_{17} phase together with the $SmFe_2$ and $SmFe_3$ phases when annealed for 0.1 h or 0.3 h, but consisted of the Sm_5Fe_{17} and $SmFe_3$ phases when annealed for 1 h. The specimens annealed at 1073 K also consisted of Sm_5Fe_{17} and $SmFe_3$ phases when annealed for 0.1 h or 0.3 h, but consisted mostly of the equilibrium Sm_2Fe_{17} and $SmFe_3$ phases when annealed for 1 h. Annealing at 1073 K for 1 h resulted in a decrease in the amount of the Sm_5Fe_{17} phase.

4. Conclusions

The crystallization behavior of an amorphous Sm_5Fe_{17} melt-spun ribbon was studied by XRD, VSM and thermomagentic valance. Although the evaluation of the crystalline phases in the annealed melt-spun ribbon was quite difficult by XRD studies, it was found to be possible by TMA studies using a thermomagnetic balance. It was also found that the specimens annealed at temperatures between 873 K and 1073 K for 0.1–1 h contained some Sm_5Fe_{17} phase, but the specimen annealed at 873 K for 1 h consisted mostly of the Sm_5Fe_{17} phase. The other annealed specimens contained other phases such as the $SmFe_2$, $SmFe_3$, Sm_2Fe_{17} phases depending on the annealing conditions.

Acknowledgment

This work was supported by a Grant-in-Aid for Scientific Research (No. 19018023) from the Japan Society for the Promotion of Science. The author would like to thank Mr. Takeshi Nishiuchi of Hitachi Metals, Ltd. for the TMA analysis.

REFERENCES

1) M. Sagawa, S. Fujimura, N. Togawa, H. Yamamoto and Y. Matsuura: J. Appl. Phys. **55** (1984) 2083–2087.
2) J. J. Croat, J. F. Herbst, R. W. Lee and F. E. Pinkerton: J. Appl. Phys. **55** (1984) 2078–2082.
3) G. C. Hadjipanayis, A. Tsoukatos, J. Strzeszewski, G. J. Long and O. A. Pringle: J. Magn. Magn. Mater. **78** (1989) L1–L5.
4) J. M. Moreau, L. Paccard, J. P. Nozieres, F. P. Missell, G. Schneider and F. J. G. Landgraf: J. Less-Common Met. **163** (1990) 245–251.
5) T. Saito, S. Ozawa and T. Motegi: J. Appl. Phys. **91** (2002) 8828–8830.
6) F. J. G. Landgraf, F. P. Missell, H. R. Rechenberg, V. Villas-Boas, J. M. Moreau, L. Paccard and J. P. Nozières: J. Appl. Phys. **70** (1991) 6125–6127.
7) F. J. Cadieu, H. Hegde, R. Rani, A. Navarathna and K. Chen: Mater. Lett. **11** (1991) 284–285.
8) R. Rani, H. Hegde, A. Navarathna, K. Chen and F. J. Cadieu: IEEE Trans. Magn. **28** (1992) 2835–2837.
9) T. Saito: J. Alloys Compd. **440** (2007) 315–318.
10) T. Saito and M. Ichihara: Scripta Mater. **57** (2007) 457–460.
11) T. Saito, I. Oguro and M. Ichihara: J. Appl. Phys. **101** (2007) 023914.
12) L. X. Liao and Z. Altounian: J. Appl. Phys. **66** (1989) 768–771.
13) K. H. J. Buschow, D. B. de Mooij and H. M. Van Noort: J. Less-Common Met. **125** (1986) 135–146.
14) D. Turnbull: Metall. Trans. A **12A** (1981) 695–708.
15) K. N. Ishihara, M. Maeda and P. H. Shingu: Acta Metall. **33** (1985) 2113–2217.
16) K. H. J. Buschow: J. Less-Common Met. **25** (1971) 131–134.